DOI: 10.1002/ejic.200500785

Heterobimetallic Ruthenium-Cobalt Complexes Containing the Pentamethylcyclopentadienyl or Indenyl Ligand

Sin Yee Ng,[a] Lai Yoong Goh,*[a] Lip Lin Koh,[a] Weng Kee Leong*[a] Geok Kheng Tan,[a] Suming Ye,[b] and Yinghuai Zhu[b]

Keywords: Heterometallic complexes / Ruthenium / Cobalt / Phosphanes / Indenyl

The salt elimination reaction between $NaCo(CO)_4$ and the ruthenium complexes LRu(diphos)Cl and [(Ind)$Ru(CO)_2Cl$] afforded the Ru–Co bimetallic complexes [$LRu(\mu\text{-}CO)_2(\mu\text{-}diphos)Co(CO)_2$] [L = C_5Me_5 (Cp^*), diphos = $Ph_2P(CH_2)_nPPh_2$, **3a**: n = 1 , or **3b**: n = 2; **3**: L = C_9H_7 (Ind), diphos = $Ph_2PCH_2PPh_2$] and [(Ind)$Ru(CO)_2Co(CO)_4$] (**3d**), respectively, in high yields. However, the same reaction with the monophosphane analogue, [(Ind)$Ru(PPh_3)_2Cl$], gave the heterobimetallic complex [(Ind)$Ru(PPh_3)(CO)(\mu\text{-}CO)Co(CO)_3$] (**3e**) in fair yield, together with redox-initiated derivatives $Ru(PPh_3)_2(CO)_3$ (**4e**) and [(Ind)$Co(CO)(PPh_3)$] (**6e**). A similar redox process in the reaction of the dppf analogue, [(Ind)Ru(dppf)Cl] (dppf = 1,1′-diphenylphosphanylferrocene) gave [Ru(dppf)$(CO)_3$] (**4f**) and [(Ind)$Co(CO)_2$] (**6f**), together with a complex salt [(Ind)Ru(dppf)(CO)][$Co(CO_4)$] [**5f·Co(CO)$_4$**].

Introduction

There has been much research activity on the employment of heterobimetallic complexes in catalysis.[1] The prime motivation for this has been the possibility of cooperative reactivity of adjacent heterometallic centres, which may impart new reactivity patterns significantly different from those of the homobimetallic complexes. Early reports of the superb catalytic efficacy of mixtures of cobalt and ruthenium compounds,[2] and later of ruthenium-cobalt heterobimetallic complexes,[2e] in methanol homologation, had spurred a surge in synthetic and reactivity studies of these complexes.[3,4] When supported on silica, they have also been found to be effective catalysts in hydroformylation.[5]

Synthetic routes to metal–metal bonded heterobimetallic complexes are very well documented;[6] one of the most commonly employed being the displacement of a halide ligand by an anionic metal fragment such as $[Co(CO)_4]^-$. Nevertheless, ruthenium-cobalt heterobimetallic complexes containing a half-sandwich ruthenium moiety have been relatively less studied. Ligands such as cyclopentadienyl (Cp) or Cp* often confer stability on the complexes, and when derivatised can effect changes in properties at the metal centre. The indenyl ligand is of much interest on account of its "indenyl effect", which is primarily a reflection of the ligand's ability to undergo $\eta^5 \leftrightarrow \eta^3$ ring slippage, thereby creating a vacant site on the metal centre without any ligand dissociation. Most of the reported compounds of this class were isolated in low yields, e.g., [(*p*-cymene)Ru$(CO)(\mu_2\text{-}PPh_2)Co(CO)_3$] (30% yield),[3d] [$CpRu(CO)_2$-$Co(CO)_4$] (10% yield),[3a] [$CpRu(PPh_3)_2Co(CO)_4$] (28% yield),[2e] and [$CpRuCo(CO)_3$(R-DAB)] (R = *i*Pr, *t*Bu, DAB = 1,4-diaza-1,3-butadiene) (10% yield).[3f] However, Matsuzaka et al. managed to isolate [$Cp^*Ru(CO)_2(\mu_2\text{-}CO)$-$Co(CO)_3$] in high yield (86%);[3h,7] subsequent substitution by dppm, *t*BuNC and alkynes (HC≡CTol, HC≡CCO_2Me) in the presence of $Me_3NO{\cdot}2H_2O$ gave very high yields of the substituted products.

In this paper, we present results from the reactions of various Cp* and Ind complexes of ruthenium with $NaCo(CO)_4$ (**1**), which gave in addition to the anticipated Ru–Co metal–metal bonded complexes, derivatives arising from redox pathways.

Results and Discussion

Salt elimination reactions between $NaCo(CO)_4$ (**1**), and the ruthenium complexes LRu(diphos)Cl (**2**) [L = Cp*, diphos = $Ph_2P(CH_2)_nPPh_2$, **2a**: n = 1 , or **2b**: n = 2; **2c**: L = Ind, diphos = $Ph_2PCH_2PPh_2$], at room temperature afforded Ru–Co bimetallic complexes [$LRu(\mu\text{-}CO)_2(\mu\text{-}diphos)$-$Co(CO)_2$] (**3**), in 78–85% yields (Scheme 1). The displacement of the halide ligand by the anionic metal fragment $[Co(CO)_4]^-$ is accompanied by the bridging of the diphosphane and two carbonyl ligands across the Ru–Co bond. We note that while [(Ind)$Ru(CO)_2Cl$] (**2d**) reacted with **1** to give the metal–metal bonded complex **3d**, $Cp^*Ru(CO)_2Cl$

[a] Department of Chemistry, National University of Singapore, 3 Science Drive 3, Singapore 117543
[b] Institute of Chemical and Engineering Sciences, 1 Pesek Road, Jurong Island, Singapore 627833

(**2d**′) gave a monocarbonyl-bridged complex **3e**′ (the prime refers to previously reported complexes), which could be decarbonylated to produce **3a** (Scheme 2).[3h]

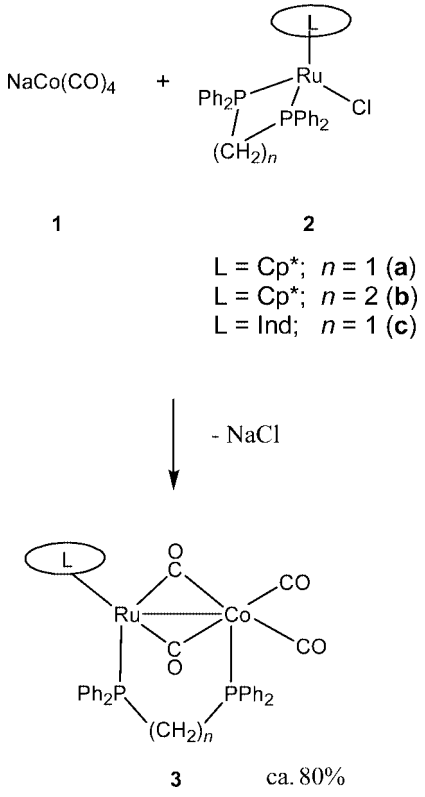

Scheme 1.

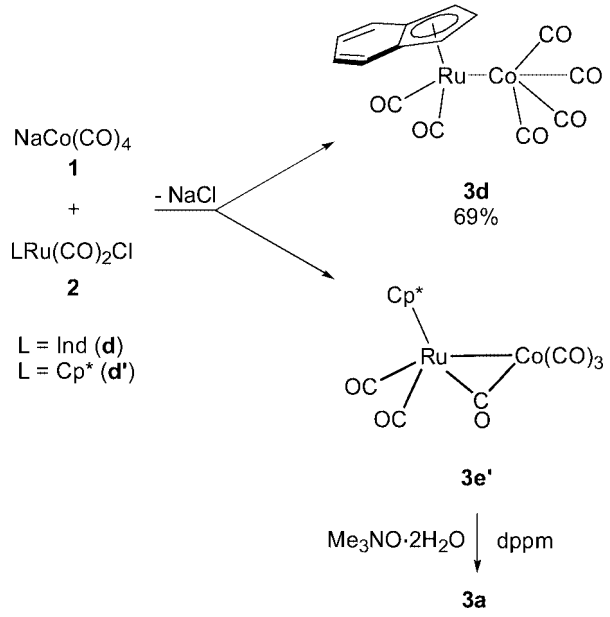

Scheme 2.

The complexes **3a**–**c** exhibited the expected resonances for the diphosphanes and Cp* or indenyl ligands in their ^{1}H NMR spectra. Their ^{31}P{^{1}H} NMR spectra all showed a sharp doublet and a broad doublet at lower field; the latter due to quadrupolar coupling to the cobalt. The IR spectra indicated the presence of both terminal and bridging carbonyls. Complex **3c** has also been characterized by a single-crystal X-ray structural study (Figure 1); that for **3a** has already been reported.[3h] Their molecular structures are very similar in that both comprise a bimetallic complex in which the ruthenium and cobalt atoms are connected by a metal–metal bond, two bridging CO ligands and a bridging diphos ligand. The Ru–Co bond length in **3c** is shorter than that in **3a** [2.6474(4) and 2.677(2) Å, respectively] and probably reflects the weaker indenyl-ruthenium compared to the Cp*–ruthenium interaction; stronger interaction in the latter would be expected to lengthen the metal–metal bond via a *trans* influence. The metal–phosphane bond lengths in both **3a** and **3c** are shorter to cobalt than to ruthenium [Ru(1)–P(3) = 2.3048(6) Å and Co(2)–P(4) = 2.2199(7) Å for **3c**]; these are comparable to the Co–P bond length of 2.175(1) Å in $Co_2(CO)_6(PMe_3)_2$,[8] and the Ru–P bond length of 2.385 Å in $\{Ru_2(CO)_4(PMe_3)_2(\mu\text{-}O_2CCH_2CO_2)\}_2$,[9] and suggest that the difference is due to the different formal oxidation states [Co(0) vs. Ru^{I}] since ruthenium and cobalt have the same covalent radii (1.26 Å). However, the reverse situation seems to be the case with regard to the bridging carbonyls.

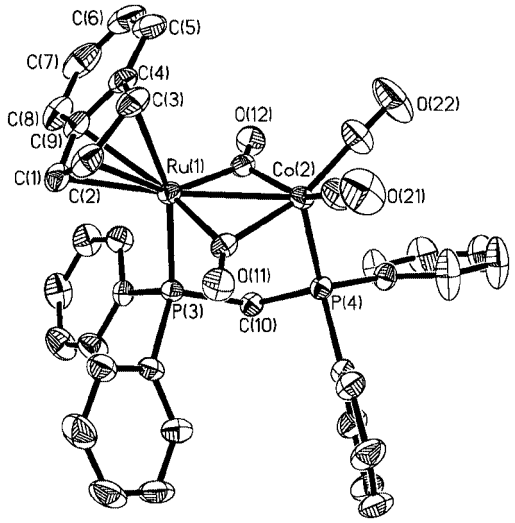

Figure 1. ORTEP diagram (50% probability thermal ellipsoids, hydrogen atoms omitted) and selected bond lengths [Å] and angles [°] of **3c**. Ru(1)–Co(2) = 2.6474(4); Ru(1)–P(3) = 2.3048(6); Co(2)–P(4) = 2.2199(7); Ru(1)–C(11) = 1.947(3); Ru(1)–C(12) = 1.962(3); Co(2)–C(22) = 1.772(3); Co(2)–C(21) = 1.776(3); Co(2)–C(12) = 2.002(3); Co(2)–C(11) = 2.021(3); O(11)–C(11) = 1.170(3); O(12)–C(12) = 1.182(3); O(21)–C(21) = 1.144(4); O(22)–C(22) = 1.130(4); P(3)–Ru(1)–Co(2) = 92.116(18); P(4)–Co(2)–Ru(1) = 99.16(2); Ru(1)–C(11)–Co(2) = 83.69(10); Ru(1)–C(12)–Co(2) = 83.80(10).

The IR spectrum of [(Ind)Ru(CO)$_2$Co(CO)$_4$] (**3d**) showed clearly the absence of any bridging carbonyl ligand, in contrast to that for the Cp* analogue **3e**′. This may be attributed to the greater electron donating ability of Cp* compared to Ind,[3h] and hence the tendency for the carbonyl ligands to bridge. This tendency is further enhanced by phosphane substitution at the metal centres, as observed in **3a**–**3c**.

The analogous reaction of the monophosphane-substituted derivative [(Ind)Ru(PPh_3)$_2$Cl] (**2e**), however, was more complex (Scheme 3). In addition to the expected heterobimetallic product [(Ind)Ru(PPh_3)(CO)(μ_2-CO)Co(CO)$_3$] (**3e**), there were the mononuclear complexes Ru(PPh_3)$_2$-(CO)$_3$ (**4e**), and [(Ind)Co(CO)(PPh_3)] (**6e**). These three compounds have been characterized completely, including by single-crystal X-ray crystallographic studies which confirmed that exchange of CO and PPh_3 ligands had occurred between the metal centres. The structure of **4e** determined here in the form of its CH_2Cl_2 solvate is essentially similar to that of its THF solvate reported previously.[10] The molecular structures of **3e** and **6e** are shown in Figure 2 and Figure 3, respectively.

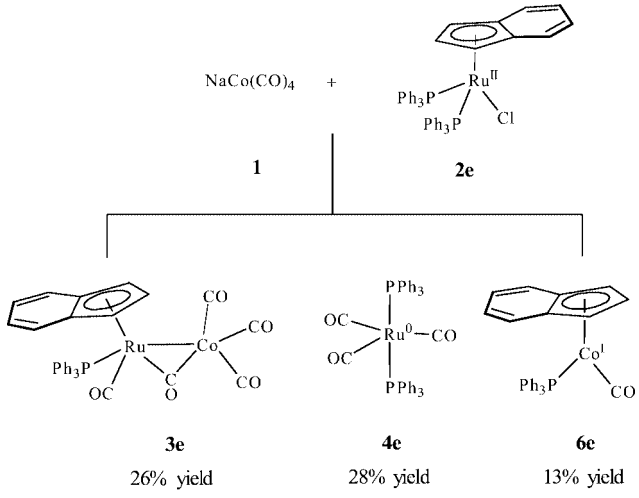

Scheme 3.

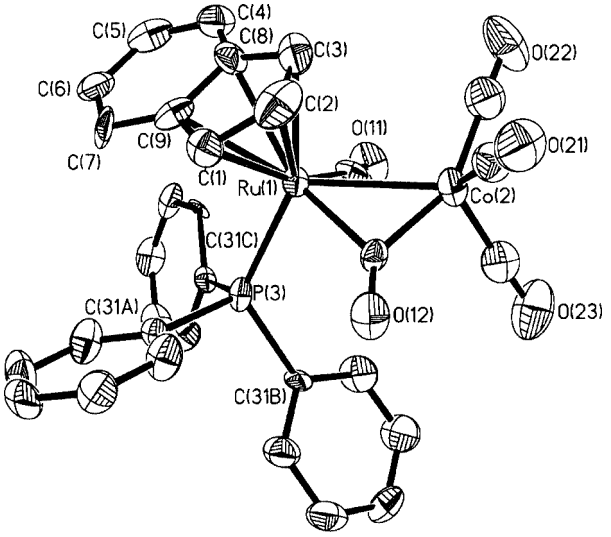

Figure 2. ORTEP diagram of **3e** (50% probability thermal ellipsoids, hydrogen atoms omitted).

There is no known Cp or Cp* analogue to **3e**. However, it is interesting to compare its structure with those of the previously reported Cp* parent carbonyl [Cp*Ru(CO)$_2$(μ-CO)Co(CO)$_3$] (**3e′**) and its isocyanide derivative [Cp*Ru(CNBu^t)(CO)(μ-CO)Co(CO)$_3$] (**3f′**);[3h] a common

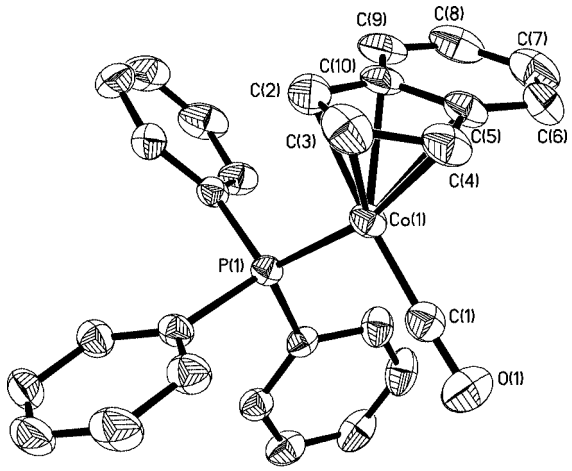

Figure 3. ORTEP diagram (50% probability thermal ellipsoids, hydrogen atoms omitted) and selected bond lengths [Å] and angles [°] of **6e**. Co(1)–C(1) = 1.711(3); Co(1)–P(1) = 2.1459(7); O(1)–C(1) = 1.156(3); C(1)–Co(1)–P(1) = 95.39(9); O(1)–C(1)–Co(1) = 176.3(3).

atomic numbering scheme and selected bond parameters are collected in Table 1. The overall structural features of the three compounds are the same, comprising of a single carbonyl bridging the Ru–Co bond, a terminal carbonyl on the ruthenium, and three on the cobalt. As in the case of **3c**, the Ru–Co bond length for **3e** is significantly shorter than in either of the Cp* analogues [2.677(2) vs. 2.7445(6) and 2.735(4) Å in **3e**, **3e′** and **3f′**, respectively]. The bridging carbonyl is obviously skewed towards the cobalt in all three compounds, as in the case of **3c**. Although there appears to be only one bridging carbonyl in these three compounds, in contrast to two for **3a** and **3c**, the carbonyl which should have made up the second bridging carbonyl [CO(11)] is actually semi-bridging [$\angle$Ru–C(11)–O(11) $\approx$ 167–169°, compared with $\angle$Co–C–O $\approx$ 173–179°].[11] This can be attributed to the presence of an electron-donating phosphorus on cobalt in the case of **3a** and **3c**, which increased electron density on the cobalt and hence the propensity towards bridging carbonyl.[12]

The molecular structure of **6e** is similar to those of known cyclopentadienyl analogues such as [CpCo(CO)$_2$],[13] and [Cp*Co(CO)$_2$],[14] and substituted indenyl analogues such as [(η^5-C$_9$H$_3$Me$_4$)Rh(CO)$_2$],[15] and [(η^5-C$_9$H$_6$CHPh$_2$)-Rh(CO)(P*i*Pr$_3$)].[16] The indenyl ligand is coordinated unsymmetrically to the Co centre, as indicated by the longer bond lengths (by $\approx$ 0.1 Å) from the metal to the bridgehead carbons than to the other three carbons of the five-membered ring. The values of the slip-fold parameters: slip distortion, Δ = 0.12(3) Å; hinge angle, HA = 5.6°; and fold angle, FA = 5.3°, are in agreement with η^5 coordination of the indenyl.[15,17]

The presence of the complexes **4e** and **6e** indicated that ligand exchange and redox reaction between the ruthenium and cobalt precursors had occurred. While the oxidation state of Ru has been reduced from +2 to 0 in **4e**, that for Co has been increased from –1 to +1 in **6e**; the ruthenium complex has also lost its indenyl and phosphane ligands in

Table 1. Common atomic numbering scheme and selected bond parameters for **3e**, **3e′** and **3f′**.

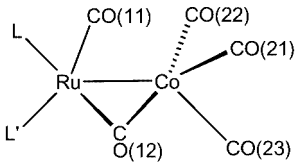

L = Ind; L' = PPh_3 **3e**
L = Cp*; L' = CO **3e'**
L = Cp*; L' = CN*t*Bu **3f'**

Bond lengths [Å] or angles [°]	**3e**	**3e′**	**3f′**
Ru–Co	2.677(2)	2.7445(6)	2.735(4)
Ru–L[a]	2.319(4)	1.890(4)	1.94(3)
Ru–C(11)	1.929(14)	1.899(4)	1.92(3)
Ru–C(12)	2.030(12)	2.206(3)	2.10(3)
Co–C(12)	1.877(14)	1.817(4)	1.83(3)
C(11)–O(11)	1.105(16)	1.136(4)	1.11(3)
C(12)–O(12)	1.186(16)	1.174(4)	1.20(3)
Co–Ru–L[a]	115.12(11)	103.7(1)	101.7(8)
Ru–C(11)–O(11)	167.2(15)	168.6(3)	168(2)
Ru–C(12)–O(12)	135.5(11)	126.0(3)	127(2)
Co–C(12)–O(12)	138.0(11)	148.5(3)	145(3)

[a] Refers to centroid of the five-membered ring.

exchange for three carbonyls. This result was in sharp contrast with the reported chemistry of the Cp analogue, for which the heterobimetallic complex, viz., $[CpRu(PPh_3)_2Co(CO)_4]$ was isolated in low yield from the reaction of $[CpRu(PPh_3)_2Cl]$ with $TlCo(CO)_4$, but on switching from the Tl^+ to the Na^+ salt, the complex salt $[CpRu(PPh_3)_2(CO)][Co(CO)_4]$ was isolated instead.[3e] Neither the displacement of PPh_3 by CO, nor the redox products that we have observed, were reported in these reactions.

Similar redox chemistry was also observed in the case of [(Ind)Ru(dppf)Cl] (**2f**). However, the heterobimetallic complex was not isolated and instead the complex salt [(Ind)-Ru(dppf)(CO)][$Co(CO_4)$] (**5f·[Co(CO)$_4$]**) was obtained, together with the Ru^0 complex $[Ru(dppf)(CO)_3]$ (**4f**) and the known Co^I complex $[(Ind)Co(CO)_2]$ (**6f**) (Scheme 4).[18] The IR spectrum of **4f** exhibited three CO stretching bands (2007, 1924 and 1896 cm^{-1}), as opposed to one (1896 cm^{-1}) for **4e**. This indicated that they have different symmetries, as was confirmed by an X-ray crystallographic study on **4f** (Figure 4). Complex **4f** adopts a distorted trigonal bipyramidal geometry at the ruthenium atom. The two phosphorus atoms of the diphos occupy an axial [P(1)] and an equatorial position [P(2)].

However, the ^{31}P NMR spectrum of **4f** showed only a singlet at δ = 40.8 ppm, implying fluxionality, as may be expected for a five-coordinate complex. Complex **5f·[Co(CO)$_4$]** was characterized spectroscopically and analytically. Its IR spectrum showed two carbonyl stretches at 1972 and 1889 cm^{-1}; very similar to the values for $[CpRu(PPh_3)_2(CO)][Co(CO)_4]$ ($\tilde{\nu}_{CO}$ = 1978 and 1872 cm^{-1}).[3e] The cation showed up as a molecular ion in the positive mode of the FAB-MS at *m*/*z* 799, together with fragments corresponding to subsequent loss of a CO and an indenyl ligand, while the anion appeared in the negative mode at *m*/*z* 171.

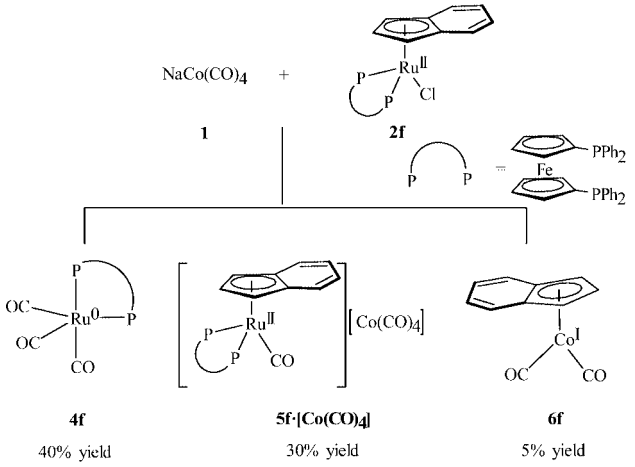

Scheme 4.

The failure to form the heterobimetallic complex at all in this case was intriguing. We have found that the halide ligand in **2f** could not be substituted by CO in a direct reaction to form [(Ind)Ru(dppf)(CO)]Cl (**5f·Cl**); a mixture of products which were not characterized was obtained instead. However, stirring **2f** under 1 atm of CO and in the presence of $NaPF_6$ afforded **5f·PF$_6$** in high yield; the same product could also be obtained from the reaction of the solvated complex $[(Ind)Ru(dppf)(NCCH_3)]PF_6$ (**7**) with 1 atm of CO (Scheme 5). We therefore believe that in the reaction between **2f** and **1**, the Cl^- ligand was abstracted and this was replaced by the coordination of CO originating from the decomposition of $[Co(CO)_4]^-$. It is this coordination of CO to the Ru centre which inhibits formation of a Ru–Co bond, presumably because of the reduced electrophilicity.

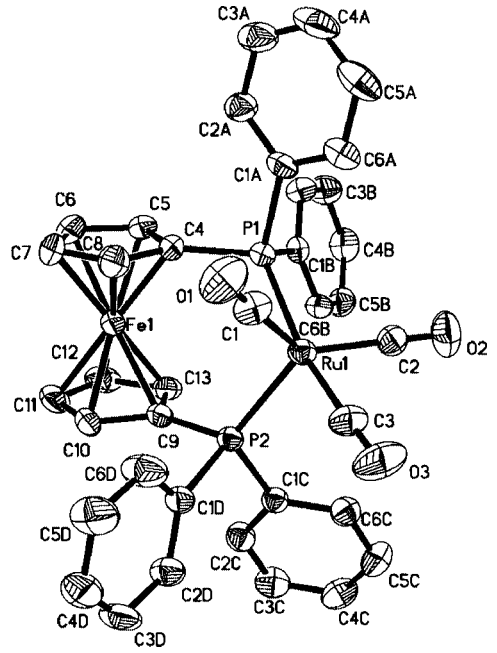

Figure 4. ORTEP diagram (50% probability thermal ellipsoids, hydrogen atoms omitted) and selected bond lengths [Å] and angles [°] of **4f**. Ru(1)–C(3) = 1.899(4); Ru(1)–C(1) = 1.902(4); Ru(1)–C(2) = 1.912(4); Ru(1)–P(1) = 2.3737(9); Ru(1)–P(2) = 2.3957(9); O(1)–C(1) = 1.150(4); O(2)–C(2) = 1.148(4); O(3)–C(3) = 1.133(4); C(3)–Ru(1)–C(1) = 88.53(16); C(3)–Ru(1)–C(2) = 87.62(16); C(1)–Ru(1)–C(2) = 135.35(16); C(3)–Ru(1)–P(1) = 168.31(12); C(1)–Ru(1)–P(1) = 86.86(12); C(2)–Ru(1)–P(1) = 88.12(11); C(3)–Ru(1)–P(2) = 94.04(12); C(1)–Ru(1)–P(2) = 110.63(12); C(2)–Ru(1)–P(2) = 114.01(12); P(1)–Ru(1)–P(2) = 97.63(3).

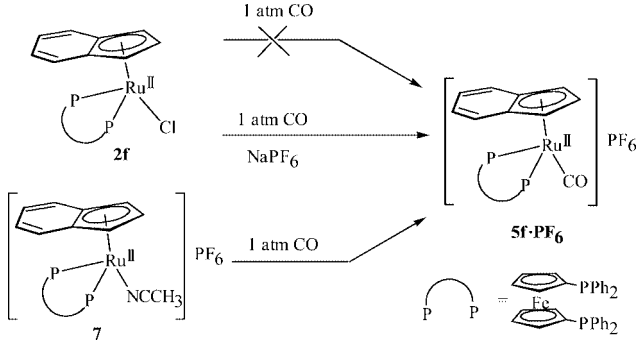

Scheme 5.

Concluding Remarks

The results above clearly show that the salt elimination reaction between $NaCo(CO)_4$ and Cp* or indenyl ruthenium chloride complexes do not always lead simply to a heterobimetallic species. The nature of the products depends on the nature of the ligands on ruthenium; in some cases, there are redox processes involved. Unfortunately, no clear trend is discernible yet as to when redox processes can become important although it would appear that a suitable diphosphane that can bridge across the heterometallic metal–metal bond is important for stabilization of the heterobimetallic product.

Experimental Section

General Procedures: All reactions were performed under dry nitrogen using Schlenk techniques or under argon in a Braun Labmaster 130 glovebox. Chromatographic separations were performed inside the glovebox. ^1H, $^{31}P\{^1H\}$ and $^{13}C\{^1H\}$ NMR spectra were recorded with a Bruker ACF300 NMR spectrometer, with chemical shifts referenced to residual non-deuterio solvent and external H_3PO_4, respectively. IR spectra were obtained as either KBr pellets or as a solution with a Shimadzu Prestige-21 FTIR-8400S spectrometer. Mass spectra were obtained with either a Finnigan MAT95XL-T (FAB) or a Finnigan MAT LCQ (ESI) spectrometer. All elemental analyses were performed by the Microanalytical Laboratory in NUS. The complexes **1**[19] and **2a**–**f**,[20] were prepared according to published methods. All other reagents are commercially available and used without further purification. All solvents were distilled from standard drying agents before use.

Reaction of $NaCo(CO)_4$ with [Cp*Ru{$Ph_2P(CH_2)_nPPh_2$}Cl] (n = 1, 2): To a THF (10 mL) solution of [Cp*Ru($Ph_2PCH_2PPh_2$)Cl] (**2a**) (100 mg, 0.15 mmol) was added a solution of $NaCo(CO)_4$ (**1**) in THF (1 equiv. in 5 mL) by cannula transfer, and the solution was refluxed for 40 h. The solvent was then removed in vacuo and the resulting residue extracted with CH_2Cl_2. Removal of the solvent gave an orange-red solid which was recrystallized from THF/hexane to afford [Cp*Ru(μ-$CO)_2$(μ-$Ph_2PCH_2PPh_2$)$Co(CO)_2$] (**3a**) as red crystals. Yield 102 mg (85%). IR (KBr, cm^{-1}): $\tilde{\nu}_{CO}$ = 1973 s, 1913 s, 1784 w, 1721 s (lit. values:[3h] (THF) $\tilde{\nu}_{CO}$ = 1985 s, 1923 s, 1728 m). ^1H NMR (300 MHz, $CDCl_3$): δ = 1.60 (s, 15 H, Cp*), 2.14 (t, 2 H, PCH_2P), 7.20–7.37 (m, 20 H, Ph) ppm. $^{31}P\{^1H\}$ NMR: δ = 55.8 (d, $^2J_{PP}$ = 103 Hz, Ru–P), 43.5 (br. s, Co–P) ppm. MS (ESI): m/z (%) = 791 $[M]^+$, 677 $[M - Co(CO)_2]^+$. $C_{39}H_{37}CoO_4P_2Ru$: C 59.2, H 4.7; formula mass 791.67; found C 59.2, H 5.2. The residue from a similar reaction between **1** and [Cp*Ru{$Ph_2P(CH_2)_2PPh_2$}Cl] (**2b**) was dissolved in a minimum volume of THF for chromatographic separation on silica gel. The main fraction (eluent: hexane/THF, 5.5:1, v/v) gave [Cp*Ru(μ-$CO)_2${μ-$Ph_2P(CH_2)_2PPh_2$}$Co(CO)_2$] (**3b**) as an orange-red solid. Yield 94 mg (78%). IR (KBr, cm^{-1}): $\tilde{\nu}_{CO}$ = 1978 s, 1920 s, 1771 w, 1722 s. ^1H NMR (300 MHz, $CDCl_3$): δ = 1.60 (s, 15 H, Cp*), 2.04, 1.84 (m, 4 H, PCH_2CH_2P), 7.19–7.68 (m, 20 H, Ph) ppm. $^{31}P\{^1H\}$ NMR: δ = 45 (s, Ru–P), 34.6 (br. s, Co–P) ppm. MS (ESI): m/z (%) = 806 $[M]^+$, 778 [M – CO], 691 $[M - Co(CO)_2]^+$. $C_{40}H_{39}CoO_4P_2Ru$: calcd. C 59.6, H 4.9; formula mass 805.70; found C 59.9, H 5.2.

Reaction of 1 with [(Ind)Ru($Ph_2PCH_2PPh_2$)Cl]: To a THF (10 mL) solution of [(Ind)Ru($Ph_2PCH_2PPh_2$)Cl] (**2c**) (100 mg, 0.13 mmol) was added **1** (1 equiv.) and the solution was stirred at room temp. for 24 h. The solvent was removed under reduced pressure, and the residue was first washed with hexane, followed by extraction with toluene. The toluene extract was concentrated and loaded onto a silica gel column prepared in *n*-hexane. Elution with toluene gave a reddish brown band as the major eluate which afforded [(Ind)Ru(μ-$CO)_2$(μ-$Ph_2PCH_2PPh_2$)$Co(CO)_2$] (**3c**). Yield 97 mg (80%). IR (CH_2Cl_2, cm^{-1}): $\tilde{\nu}_{CO}$ = 1997 s, 1944 s, 1739 s. ^1H NMR (300 MHz, C_6D_6): δ = 2.03 [t, J = 9.06 Hz, 2 H, $CH_2(PPh_2)_2$], 5.18–5.20 (m, 3 H, η^5-C_9H_7), 6.64–6.67, 6.89–7.01, 7.10–7.14, 7.30–7.36 [m, 24 H, $CH_2(PPh_2)_2$ and η^5-C_9H_7] ppm. $^{31}P\{^1H\}$ NMR: δ = 44.4 (br. d, $^2J_{PP}$ = 109 Hz, Co–P), 59.3 (d, $^2J_{PP}$ = 109 Hz, Ru–P) ppm. MS (FAB^+): m/z (%) = 716 $[M - 2CO]^+$, 657 $[M - 2CO - Co]^+$, 629 $[M - 3CO - Co]^+$, 601 $[M - 4CO - Co]^+$. $C_{38}H_{29}CoO_4P_2Ru$: calcd. C 59.2, H 3.8; formula mass 771.60; found C 59.6, H 3.4.

For the reaction with [(Ind)$Ru(CO)_2$Cl] (**2d**) (30 mg, 0.098 mmol), the hexane extract was concentrated and cooled to –30 °C for 1 day

to give [(Ind)Ru(CO)$_2$Co(CO)$_4$] (**3d**) (30 mg, 69%) as dark red crystals.

For 3d: IR (hexane, cm^{-1}): $\tilde{\nu}_{CO}$ = 2067 m, 2022 s, 1986 m, br., 1963 w, br., 1955 w, br. ^{1}H NMR (300 MHz, C_6D_6): δ = 4.60 (t, $^3J_{HH}$ = 3.3 Hz, 1 H, η^5-C_9H_7), 4.81 (d, 2 H, η^5-C_9H_7), 6.79 (s, 4 H, η^5-C_9H_7) ppm. ^{13}C NMR (75 MHz, C_6D_6): δ = 76.5 (s, C1,3), 91.5 (s, C2), 111.1 (s, C8,9), 124.2 and 129.8 (s, C4–7), 204.3 (CO) ppm. MS (FAB$^+$): *m/z* (%) = 444 [M]$^+$, 388 [M – 2CO]$^+$, 360 [M – 3CO]$^+$, 332 [M – 4CO]$^+$. $C_{15}H_7CoO_6Ru$: calcd. C 40.7, H 1.6; formula mass 443.22; found C 40.8, H 1.5.

For the reaction with [(Ind)Ru(PPh$_3$)$_2$Cl] (**2e**), the toluene extract was concentrated and chromatographed on a silica gel column. Elution gave four fractions: (i) A yellow eluate with hexane/toluene (4:1, v/v) yielded [(Ind)Co(CO)(PPh$_3$)] (**6e**) (8 mg, 13%) as air-sensitive dark red crystals after recrystallization from CH_2Cl_2/hexane; (ii) an orange-yellow eluate (severe tailing) with hexane/toluene (3:1, v/v) gave [Ru(PPh$_3$)$_2$(CO)$_3$] (**4e**) after several recrystallizations from toluene/hexane (1:4, v/v) (26 mg, 28%); (iii) a reddish brown eluate with hexane/toluene (1:1, v/v) yielded [(Ind)-Ru(PPh$_3$)(CO)(μ_2-CO)Co(CO)$_3$] (**3e**) (23 mg, 26%); and (iv) a red eluate with toluene/THF (1:1, v/v) afforded unreacted **2e** (20 mg, 20%).

For 3e: IR (CH_2Cl_2, cm^{-1}): $\tilde{\nu}_{CO}$ = 1975 s, 1920 s, 1744 m. ^{1}H NMR (300 MHz, C_6D_6): δ = 4.98 (s, 3 H, η^5-C_9H_7), 6.57–6.93 (m, 4 H, η^5-C_9H_7), 7.03–7.72 (m, 15 H, PPh$_3$) ppm. ^{31}P{^{1}H} NMR: δ = 48.6 (s, PPh$_3$) ppm. MS (FAB$^+$): *m/z* (%) = 566 [M – 4CO]$^+$, 535 [M – Co – 3CO]$^+$, 479 [M – Co – 5CO]$^+$. $C_{32}H_{22}CoFeO_5P{\cdot}2C_6H_5CH_3$: calcd. C 64.4, H 4.0; formula mass 816.56; found C 64.1, H 4.2. The presence of toluene solvent has been confirmed by ^{1}H NMR spectroscopy.

For 4e: IR (CH_2Cl_2, cm^{-1}): $\tilde{\nu}_{CO}$ = 1896 s (lit. values:[10b] (THF) $\tilde{\nu}_{CO}$ = 1900 s). ^{1}H NMR (300 MHz, C_6D_6): δ = 6.96–7.05 (m, 18 H, PPh$_3$), 7.87–7.93 (m, 12 H, PPh$_3$) ppm. ^{31}P{^{1}H}NMR: δ = 55.9 (s, PPh$_3$) ppm.

For 6e: IR (KBr, cm^{-1}): $\tilde{\nu}_{CO}$ = 1922 s. ^{1}H NMR (300 MHz, C_6D_6): δ = 4.61 (s, 2 H, η^5-C_9H_7), 5.67 (t, $^3J_{HH}$ = 3.3 Hz, 1 H, η^5-C_9H_7), 6.74–6.78 (4-lines m, 2 H, η^5-C_9H_7), 6.94–6.97, 6.98–7.01, 7.41–7.48 (each m, total 17 H, PPh$_3$ and η^5-C_9H_7) ppm. ^{31}P NMR: δ = 65.6 (br. s, PPh$_3$) ppm. ESI$^+$-MS: 667 [2M – PPh$_3$]$^+$, 405 [2M – 2PPh$_3$]$^+$. $C_{28}H_{22}CoOP{\cdot}\frac{1}{8}CH_2Cl_2$: calcd. C 71.0, H 4.7; formula mass 475.00; found C 70.5, H 4.5. The presence of dichloromethane solvent has been confirmed by ^{1}H NMR spectroscopy.

For the reaction with [(Ind)Ru(dppf)Cl] (**2f**), extraction with toluene was followed by extraction with CH_3CN. The toluene extract was concentrated and chromatographed on a silica gel column. Elution with hexane/toluene (2:1, v/v) gave a yellow eluate of [(Ind)-Co(CO)$_2$] (**6f**). Yield 4 mg (5%). IR (CH_2Cl_2): $\tilde{\nu}_{CO}$ = 2027 and 1970 cm^{-1}; lit. values (CH_2Cl_2):[18] 2030, 1970. Further elution with hexane/toluene (4:3, v/v) afforded an orange-yellow eluate which gave [Ru(dppf)(CO)$_3$] **4f** after several recrystallizations from toluene/hexane (1:4, v/v). Yield 37 mg (40%). The CH_3CN extract gave [(Ind)Ru(dppf)(CO)][Co(CO$_4$)] (**5f·[Co(CO)$_4$]**) as a dark brown oil. Yield 36 mg (30%).

For 4f: IR (CH_2Cl_2, cm^{-1}): $\tilde{\nu}_{CO}$ = 2007 s, 1924 m, 1896 s. ^{1}H NMR (300 MHz, C_6D_6): 4.27 (s, 4 H, C_5H_4), 4.28 (s, 4 H, C_5H_4), 7.02–7.88 (m, 20 H, Ph) ppm. ^{31}P{^{1}H} NMR: δ = 40.8 (s, dppf) ppm. MS (FAB$^+$): *m/z* (%) = 740 [M]$^+$, 712 [M – CO]$^+$, 684 [M – 2CO]$^+$, 655 [M – 3CO]$^+$. $C_{37}H_{28}FeO_3P_2Ru$: calcd. C 59.9, H 3.8; formula mass 739.49; found C 60.1, H 3.8.

For 5f·[Co(CO)$_4$]: IR (CH_2Cl_2): $\tilde{\nu}_{CO}$ = 1972 m, 1889 s cm^{-1}. ^{1}H NMR (300 MHz, CD_3CN): δ = 4.37 (s, 2 H, C_5H_4), 4.46 (s, 2 H, C_5H_4), 4.57 (s, 2 H, C_5H_4), 4.61 (s, 2 H, C_5H_4), 5.25 (s, 3 H, η^5-C_9H_7), 6.77–7.06 (m, 4 H, η^5-C_9H_7), 7.18–7.71 (m, 20 H, Ph) ppm. ^{31}P{^{1}H}: δ = 54.8 (s, dppf) ppm. FAB$^+$-MS: *m/z* 799 [M]$^+$, 771 [M –

Table 2. Crystal and refinement data for **3c**, **3e**, **4e**, **4f** and **6e**.

Compound	**3c**	**3e**	**4e**	**4f**	**6e**
Empirical formula	$C_{38}H_{29}CoO_4P_2Ru{\cdot}CH_2Cl_2$	$C_{32}H_{22}CoO_5PRu$	$C_{39}H_{30}O_3P_2Ru{\cdot}CH_2Cl_2$	$C_{37}H_{28}FeO_3P_2Ru$	$C_{28}H_{22}CoOP$
Formula weight	856.48	677.47	794.57	739.45	464.36
Crystal system	monoclinic	orthorhombic	triclinic	monoclinic	monoclinic
Space group	$P2_1/c$	$P2_12_12_1$	$P\bar{1}$	$P2_1/c$	$P2_1/c$
a [Å]	10.5588(5)	11.898(2)	9.9667(6)	9.7242(6)	9.1150(5)
b [Å]	16.9898(8)	15.098(3)	13.6718(8)	16.2461(10)	25.7691(15)
c [Å]	20.1273(9)	15.376(3)	15.4090(9)	19.9335(12)	10.4250(6)
α [°]	90	90	63.7400(10)	90	90
β [°]	94.3280(10)	90	87.6650(10)	95.082(2)	115.9190(10)
γ [°]	90	90	74.4430(10)	90	90
Volume [Å^3]	3600.4(3)	2762.2(9)	1806.60(18)	3136.7(3)	2202.4(2)
Z	4	4	2	4	4
Density (calculated) [Mg/m^3]	1.580	1.629	1.461	1.566	1.400
Absorption coefficient [mm^{-1}]	1.158	1.246	0.708	1.083	0.870
F(000)	1728	1360	808	1496	960
Crystal size [mm]	0.36 × 0.32 × 0.20	0.25 × 0.08 × 0.07	0.20 × 0.16 × 0.14	0.30 × 0.12 × 0.09	0.30 × 0.10 × 0.08
θ range for data collection [°]	2.28 to 30.01	2.18 to 26.37	2.34 to 27.50	1.62 to 27.50	1.58 to 27.50
Reflections collected	33154	20635	23823	18602	15374
Independent reflections	10167 [*R*(int) = 0.0303]	3171 [*R*(int) = 0.1020]	8273 [*R*(int) = 0.0430]	7202 [*R*(int) = 0.0443]	5057 [*R*(int) = 0.0375]
Max. and min. transmission	0.8014 and 0.6806	0.9178 and 0.7458	0.9074 and 0.8714	0.9088 and 0.7371	0.9337 and 0.7804
Data / restraints / parameters	10167 / 7 / 451	3171 / 30 / 361	8273 / 6 / 455	7202 / 0 / 397	5057 / 0 / 280
Goodness-of-fit on F^2	1.070	1.333	1.101	1.037	1.114
Final *R* indices [$I > 2\sigma(I)$]	R_1 = 0.0392, wR_2 = 0.1029	R_1 = 0.0889, wR_2 = 0.1779	R_1 = 0.0534, wR_2 = 0.1258	R_1 = 0.0468, wR_2 = 0.1018	R_1 = 0.0521, wR_2 = 0.1088
R indices (all data)	R_1 = 0.0498, wR_2 = 0.1154	R_1 = 0.0964, wR_2 = 0.1807	R_1 = 0.0636, wR_2 = 0.1311	R_1 = 0.0646, wR_2 = 0.1087	R_1 = 0.0694, wR_2 = 0.1152
Largest diff. peak / hole [e·Å^{-3}]	0.942 / –0.492	1.958 / –1.437	1.158 / –0.813	0.682 / –0.337	0.654 / –0.236

$CO]^+$, 655 $[M - CO - Ind]^+$. MS (FAB^-): *m/z* (%) = 171 $[Co(CO)_4]^-$. MS (HR-FAB^+): *m/z* (%) = 799.0562 (found), 799.0562 (calcd.).

Synthesis of [(Ind)Ru(dppf)(CO)]PF_6

Method A: $NaPF_6$ (5 mg, 0.03 mmol) was added to a solution of **2f** (20 mg, 0.02 mmol) in THF (10 mL). The mixture was subjected to three freeze-pump-thaw cycles, then CO (1 atm) was bubbled through the solution for about 10 min. The reaction mixture was stirred at room temp. for 24 h, during which the colour of the solution changed from red to yellow. The mixture was filtered and concentrated to ca. 2 mL. Addition of ether (5 mL) followed by cooling at –30 °C for 1 d gave [(Ind)Ru(dppf)(CO)]PF_6 (**5f·PF_6**). Yield 20 mg (85%).

Method B: A solution of **7** (20 mg, 0.02 mmol) in THF (10 mL) was degassed by three freeze-pump-thaw cycles, and then saturated with CO (1 atm; bubbling for ca. 10 min). The reaction mixture was stirred at room temp. for 24 h, filtered and then concentrated to ca. 2 mL. Addition of ether (5 mL) followed by cooling at –30 °C for 1 day gave **5f·PF_6**. Yield 17 mg (86%). IR (THF, cm^{-1}): $\tilde{\nu}_{CO}$ = 1973 s. ^1H NMR (300 MHz, CD_3CN): δ = 4.37 (s, 2 H, C_5H_4), 4.46 (s, 2 H, C_5H_4), 4.57 (s, 2 H, C_5H_4), 4.61 (s, 2 H, C_5H_4), 5.24 (s, 3 H, η^5-C_9H_7), 6.76–7.06 (m, 4 H, η^5-C_9H_7), 7.18–7.71 (m, 20 H, Ph) ppm. $^{31}P\{^1H\}$ NMR: δ = 54.8 (s, dppf), –142.9 (sept, PF_6) ppm. MS (FAB^+): *m/z* (%) = 799 $[M]^+$, 771 $[M - CO]^+$, 655 $[M - CO - Ind]^+$. MS (FAB^-): *m/z* (%) = 145 $[PF_6]^-$. $C_{44}H_{35}F_6FeOP_3Ru$: calcd. C 56.0, H 3.7; formula mass 943.59; found C 56.0, H 3.7.

Crystal Structure Determinations: Crystals were grown from dichloromethane/hexane solutions and mounted on quartz fibres. X-ray data were collected with a Bruker AXS APEX system, using Mo-K_a radiation, with the SMART suite of programs.[21] Data were processed and corrected for Lorentz and polarisation effects with SAINT,[22] and for absorption effects with SADABS.[23] Structural solution and refinement were carried out with the SHELXTL suite of programs.[24] Crystal and refinement data are summarised in Table 2. The structures were solved by direct methods or Patterson maps to locate the heavy atoms, followed by difference maps for the light, non-hydrogen atoms. All non-hydrogen atoms were generally given anisotropic displacement parameters in the final model (except for the carbon atoms of the disordered solvate in **4e**). Clusters **3c** and **4e** had one CH_2Cl_2 solvate molecule each, which exhibited disorder over two sites. For **3c**, the site occupancies were 0.75 and 0.25; for **4e**, these were 0.9 and 0.1. Appropriate restraints were placed on the atomic anisotropic parameters and bond and interatomic distances.

CCDC 283009–283013 contain the supplementary crystallographic data for this paper. These data can be obtained free of charge from The Cambridge Crystallographic Data Centre via www.ccdc.cam.ac.uk/data_request/cif.

Acknowledgments

This work was supported by an A*STAR grant (Research Grant No. 012 101 0035) and one of us (S. Y. N.) thanks the University for a Research Scholarship. Contribution from Dr. J. Zhang in the earlier part of this work is also acknowledged.

[1] a) P. Braunstein, E. W. Rose in *Comprehensive Organometallic Chemistry II* (Eds.: J. Abel, F. G. A. Stone, G. Wilkinson), Elsevier, Oxford, **1995**, vol. 10, p. 351; b) R. D. Adams, F. A. Cotton (Eds.), *Catalysis by Di and Polynuclear Metal Cluster Complexes*, Wiley-VCH, Weinheim, **1998**; c) P. Braunstein, I. Rose in *Chemical Bonds: Better Ways to Make Them and Break Them* (Ed.: I. Bernal), Elsevier, Amsterdam, **1989**, p. 89; d) G. Süss-Fink, G. Meister, *Adv. Organomet. Chem.* **1993**, *35*, 41.

[2] a) W. R. Pretzer, T. P. Kobylinski, J. E. Bozik (Gulf Research and Development Company), U. S. Patents 4133966, **1979** and 4239924, **1980**; b) R. Fiato (Union Carbide Corporation), U. S. Patent 4253987, **1980**; c) British Petroleum, Ltd, British Patent 2036739, **1980**; d) G. Doyle (Exxon Research & Engineering Company), U. S. Patent 4348541, **1982**; e) G. Doyle, *J. Mol. Catal.* **1983**, *18*, 251; f) M. Hidai, M. Orisaku, M. Ue, Y. Koyasu, T. Kodoma, Y. Uchida, *Organometallics* **1983**, *2*, 292; g) K. Watanabe, K. Kudo, N. Sugita, *Bull. Chem. Soc. Jpn.* **1985**, *58*, 2029; h) E. Santacesaria, M. Di Serio, *J. Mol. Catal.* **1990**, *58*, 43; i) K. Tominaga, Y. Sasaki, T. Watanabe, M. Saito, *Stud. Surf. Sci. Catal.* **1998**, *114*, 495.

[3] a) A. R. Manning, *J. Chem. Soc. (A)* **1971**, 2321; b) R. Regragui, P. H. Dixneuf, *J. Organomet. Chem.* **1982**, *239*, C12; c) H. C. Foley, W. C. Finch, C. G. Plerpont, G. L. Geoffroy, *Organometallics* **1982**, *1*, 1379; d) R. Regragui, P. H. Dixneuf, N. J. Taylor, A. J. Carty, *Organometallics* **1984**, *3*, 1020; e) G. Doyle, D. V. Engen, *J. Organomet. Chem.* **1985**, *280*, 253; f) R. Zoet, G. van Koten, A. L. J. van der Panne, P. Versloot, C. H. Stam, K. Vrieze, *Inorg. Chim. Acta* **1988**, *149*, 177; g) M. R. Gagné, J. Takats, *Organometallics* **1988**, *7*, 561; h) H. Matsuzaka, K. Ichikawa, T. Ishioka, H. Sato, T. Okubo, T. Ishii, M. Yamashita, S. Kondo, M. Kitagawa, *J. Organomet. Chem.* **2000**, *596*, 121.

[4] a) R. Regragui, P. H. Dixneuf, N. J. Taylor, A. J. Carty, *Organometallics* **1984**, *3*, 814; b) R. Regragui, P. H. Dixneuf, N. J. Taylor, A. J. Carty, *Organometallics* **1986**, *5*, 1; c) S. Guesmi, P. H. Dixneuf, G. Süss-Fink, N. J. Taylor, A. J. Carty, *Organometallics* **1989**, *8*, 307; d) J. N. L. Dennett, J. Jacke, G. Nilsson, A. Rosborough, M. J. Ferguson, M. Wang, R. McDonald, J. Takats, *Organometallics* **2004**, *23*, 4478.

[5] a) L. Tang, M. Huang, Y. Jiang, *Reactive Polymers* **1994**, *23*, 119; b) S. Guan, M. Huang, Y. Jiang, *Chinese J. Polymer Sci.* **1993**, *11*, 103; c) H. Zong, W. Tang, Z. Chen, Y. Jiang, *Chinese J. Polymer Sci.* **1991**, *9*, 171; d) Q. Tang, H. Zong, Z. Chen, Y. Jiang, *Chinese J. Polymer Sci.* **1991**, *9*, 39; e) S. Cao, M. Huang, Y. Jiang, *Polym. Bull.* **1988**, *19*, 353.

[6] a) D. W. Stephan, *Coord. Chem. Rev.* **1989**, *95*, 41; b) N. Wheatley, P. Kalck, *Chem. Rev.* **1999**, *99*, 3379; c) E. W. Adams in *Comprehensive Organometallic Chemistry II* (Eds.: R. D. Abel, F. G. A. Stone, G. Wilkinson), Elsevier, Oxford, **1995**, vol. 10, p. 1; d) E. W. Chetcuti in *Comprehensive Organometallic Chemistry II* (Eds.: M. J. Abel, F. G. A. Stone, G. Wilkinson), Elsevier, Oxford, **1995**, vol. 10, p. 24.

[7] H. Matsuzaka, K. Ichikawa, T. Ishii, M. Kondo, S. Kitagawa, *Chem. Lett.* **1998**, 1175.

[8] R. A. Jones, M. H. Seeberger, A. L. Stuart, B. R. Whittlesey, T. C. Wright, *Acta Crystallogr. Sect. C: Cryst. Struct. Commun.* **1986**, *42*, 399.

[9] K.-B. Shiu, H.-C. Lee, G.-H. Lee, Y. Wang, *Organometallics* **2002**, *21*, 4013.

[10] a) F. Dahan, S. Sabo, B. Chaudret, *Acta Crystallogr. C: Cryst. Struct. Commun.* **1984**, *40*, 786; b) E. M. Gordon, R. Eisenberg, *J. Mol. Catal.* **1988**, *45*, 57.

[11] R. H. Crabtree, M. Lavin, *Inorg. Chem.* **1986**, *25*, 805.

[12] P. J. Dyson, J. S. McIndoe, *Transition Metal Carbonyl Cluster Chemistry*, Gordon and Breach, Amsterdam, **2000**.

[13] M. Y. Antipin, Y. T. Struchkov, A. N. Chernega, M. F. Meidine, J. F. Nixon, *J. Organomet. Chem.* **1992**, *436*, 79.

[14] L. R. Byers, L. F. Dahl, *Inorg. Chem.* **1980**, *19*, 277.

[15] A. K. Kakkar, N. J. Taylor, T. B. Marder, J. K. She, N. Hallinan, F. Basolo, *Inorg. Chim. Acta* **1992**, *198–200*, 219.

[16] E. Bleuel, O. Gevert, M. Laubender, H. Werner, *Organometallics* **2000**, *19*, 3109.

[17] M. J. Calhorda, L. F. Veiros, *Coord. Chem. Rev.* **1999**, *185–186*, 37 and references cited therein.

[18] A. Salzer, C. Täschler, *J. Organomet. Chem.* **1985**, *294*, 261.
[19] W. F. Edgell, J. Lyford, *Inorg. Chem.* **1970**, *9*, 1932.
[20] a) M. I. Bruce, B. G. Ellis, P. J. Low, B. W. Skelton, A. H. White, *Organometallics* **2003**, *22*, 3184; b) L. A. Oro, M. A. Ciriano, M. Campo, C. Foces-Foces, F. H. Cano, *J. Organomet. Chem.* **1985**, *289*, 117; c) M. P. Gamasa, J. Gimeno, C. Gonzelz-Bernardo, B. M. Martí-Vaca, D. Monti, M. Bassetti, *Organometallics* **1996**, *15*, 302; d) S. Y. Ng, Y. Zhu, W. K. Leong, R. Webster, L. Y. Goh, manuscript in preparation.
[21] *SMART* version 5.628, Bruker AXS Inc., Madison, Wisconsin, USA, **2001**.
[22] *SAINT*+ version 6.22a, Bruker AXS Inc., Madison, Wisconsin, USA, **2001**.
[23] G. W. Sheldrick, *SADABS*, University of Göttingen, **1996**.
[24] G. W. Sheldrick, *SHELXTL*, Bruker Analytical Instruments, Madison, Version 5.1, **1997**.

Received: September 6, 2005
Published Online: December 13, 2005

